



# Predicting groundwater level fluctuations with meteorological effect implications—A comparative study among soft computing techniques

Jalal Shiri <sup>a,\*</sup>, Ozgur Kisi <sup>b</sup>, Heesung Yoon <sup>c</sup>, Kang-Kun Lee <sup>d</sup>, Amir Hossein Nazemi <sup>a</sup>

<sup>a</sup> Faculty of Agriculture, Water Engineering Department, University of Tabriz, Tabriz, Iran

<sup>b</sup> Civil Engineering Department, Faculty of Architecture and Engineering, Canik Basari University, Samsun, Turkey

<sup>c</sup> Groundwater Laboratory, Korea Institute of Geoscience and Mineral Resources (KIGAM), Korea

<sup>d</sup> School of Earth and Environmental Science, Seoul National University, Seoul, Korea

## ARTICLE INFO

### Article history:

Received 4 April 2012

Received in revised form

14 November 2012

Accepted 7 January 2013

Available online 11 February 2013

### Keywords:

Groundwater level fluctuations

Prediction

Artificial intelligence techniques

ARMA

## ABSTRACT

The knowledge of groundwater table fluctuations is important in agricultural lands as well as in the studies related to groundwater utilization and management levels. This paper investigates the abilities of Gene Expression Programming (GEP), Adaptive Neuro-Fuzzy Inference System (ANFIS), Artificial Neural Networks (ANN) and Support Vector Machine (SVM) techniques for groundwater level forecasting in following day up to 7-day prediction intervals. Several input combinations comprising water table level, rainfall and evapotranspiration values from Hongcheon Well station (South Korea), covering a period of eight years (2001–2008) were used to develop and test the applied models. The data from the first six years were used for developing (training) the applied models and the last two years data were reserved for testing. A comparison was also made between the forecasts provided by these models and the Auto-Regressive Moving Average (ARMA) technique. Based on the comparisons, it was found that the GEP models could be employed successfully in forecasting water table level fluctuations up to 7 days beyond data records.

© 2013 Elsevier Ltd. All rights reserved.

## 1. Introduction

Groundwater excluding the polar ice caps and glaciers (Raghunath, 2003) is a precious and widely distributed water resource of the earth. From a utilization perspective, agriculture (irrigation) is the greatest user of water accounting for 80% of all consumptions. Beside agricultural consumptions, groundwater is the significant source of drinking, domestic and industrial water worldwide. In order to make an effective water resources management system, it is necessary to predict groundwater level variations with acceptable accuracies. Groundwater levels are subjected to variations due to differences between the supply and release of groundwater, gaining/loosing streamflow variations, tidal effects, urbanization, earthquake, land subsidence and meteorological phenomena as well as global climatic changes (Todd and Mays, 2005). The effective meteorological phenomena in groundwater level fluctuations include atmospheric pressure (which produces considerable fluctuation in confined aquifers), wind blowing over the top of the water wells (which causes minor fluctuations in groundwater level), frost, precipitation (e.g. rainfall) and evapotranspiration. Meanwhile, rainfall causes minor

fluctuations wherever surface/subsurface losses of rainfall or travel time for vertical percolation are sizeable. However, in adequately permeable aquifers, the response of groundwater level to rainfall may be rapid, so, rainfall can be considered as a good indicator for groundwater level fluctuations in such aquifers (Todd and Mays, 2005).

So far, many investigations have been achieved to predict groundwater level fluctuations. Some of them are physically based numerical models used to characterize the groundwater flow in aquifers and some are empirical applying (Box and Jenkins, 1976 and Hipel and McLeod, 1994) models to produce time series of water table depths. However, the physically based models need a large quantity of accurate data and since the physical properties of groundwater can never be ascertained with absolute accuracy, unavoidable discrepancies between the model and the real world system reduce simulation accuracy hindering efforts to appropriately manage the groundwater resources (Coppola et al., 2005). Also the empirical time series models have their own limitations, because they are not adequate when the dynamical behavior of the hydrological system changes with time (Bierkens, 1998). In the recent years, the use of Artificial Intelligence (AI) approaches [i.e. Genetic Programming (GP), Artificial Neural Networks (ANN), Adaptive Neuro-Fuzzy Inference System (ANFIS) and Support Vector Machine (SVM) techniques] in water resources issues has become viable.

\* Corresponding author. Tel.: +98 411 334 0081.

E-mail address: j\_shiri2005@yahoo.com (J. Shiri).

In hydrologic research field, ANN models have been developed and applied to predict diverse water resources variables for an effective water management. Rizzo and Dougherty (1994) used ANNs to characterize the aquifer properties. Coulibaly et al. (2001) used ANNs for modeling of monthly groundwater level fluctuations. Coppola et al. (2005) applied ANNs for accurate prediction of potentiometric surface elevations. Nayak et al. (2006) investigated the potential of ANN for forecasting groundwater levels in an unconfined aquifer. Szidarovszky et al. (2007) introduced a hybrid ANN-numerical groundwater flow model for improving numerical model predictions by constraining the numerical solution with ANN-predicted values. Coppola et al. (2007) applied a combination of ANN modeling with multi-objective optimization for complicated real-world groundwater management problems. Yoon et al. (2007) used ANNs to forecast solute breakthrough curve in unsaturated porous media. Feng et al. (2008) applied ANNs to investigate the effects of human activities on regional groundwater levels. Also, many researchers have reported that the SVM approach is successfully applied to hydrologic problems and their performance is comparable or superior to ANN (Khalil et al., 2006; Gill et al., 2007; Yoon et al., 2010).

ANFIS technique has been applied in complex dynamic hydrological modeling (Hong and White, 2009) and groundwater depth fluctuations modeling (Kisi and Shiri, 2012).

The application of GP (i.e. Gene Expression Programming, GEP) to modeling time-series of groundwater levels is also limited. Shiri and Kisi (2011) used time series of measured groundwater levels for predicting groundwater level fluctuations.

The main purpose of the present study is to analyze the performance of the GEP, ANFIS, ANN and SVM techniques in daily water table elevation forecasting using the daily water table as well as rainfall data. The predictions of the models were compared with those of observed values using a detailed statistical analysis.

## 2. Materials and methods

### 2.1. Data analysis

In the present study, daily groundwater level ( $h$ ) and rainfall ( $R$ ) data for Hoengchon Well in Republic of Korea were deployed. Fig. 1 shows the geographical position of the studied site. Daily

groundwater level values used in this modeling exercise are the averages of 24 hourly measurements, while corresponding daily precipitation values are the total precipitation measured over the 24-h period. Automatic groundwater level loggers for the National Groundwater Monitoring Network (NGMN) are inspected and calibrated every two months to ensure high quality data. One of the objectives for installation and operation of NGMN is to establish a natural background database of groundwater levels across Korea that is not affected by pumping. Thus, most of NGMN stations have been installed in areas where the affect of groundwater extraction on groundwater level fluctuations is minimal. Therefore, this variable was not considered a relevant model input in this study. In contrast, because precipitation is the primary and most critical variable affecting short-term groundwater level fluctuations within the study area, data collected from a rainfall station located near the Hongcheon station (with distance of 500 m) was used as input to the models.

It is noted that different disciplines require the processing and applying of data at various time intervals, according to the degree of desirability and necessity for different applications. For instance, daily groundwater depth data are important in irrigation scheduling in arid and semi-arid region, where the water is scarce, especially in the period when the water consumptive use of plants are high (Shiri and Kisi, 2011).

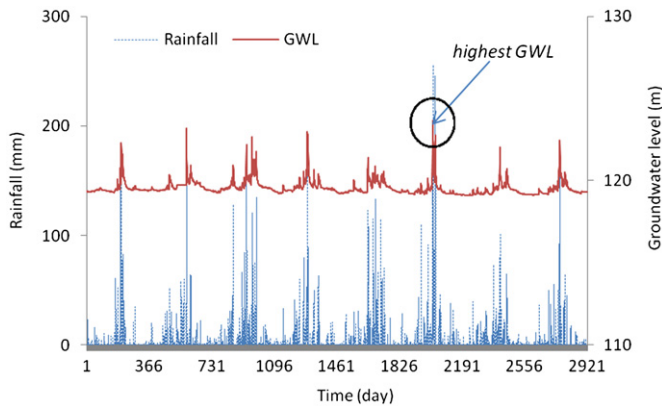
The applied data comprise the observations for eight years (from 1st January 2001 to 31st December 2008), from which those of the first six years have been used for training the applied models and the last two years have been reserved for testing. Table 1 summarizes the geographical position of the Hoengchon Well and aquifer characteristics. From the well vertical profile listed in Table 1, it is seen that the rainfall water can easily recharge the groundwater, and the response time is very short. Consequently, rainfall and evapotranspiration can be considered as a good indicator for analyzing groundwater level variations. Groundwater level data have been measured as height above the mean sea level, by using a pressure sensor. Using the meteorological data of the studied region during the same period, the potential evapotranspiration ( $ET$ ) values were calculated by global FAO56-PM model (Allen et al., 1998). Fig. 2 displays the observed time series of groundwater level and rainfall during the study period. From the figure it can be observed that the highest groundwater level (during the study period) occurs in the 17th



Fig. 1. Map of situation of the studied site (Hongcheon Station- Korea).

**Table 1**  
Summary of the studied station.

Location	Hongcheon
Latitude (°N)	37° 41' 20.2"
Longitude (°E)	127° 52' 29.0"
Altitude (meters above mean sea level)	128.536
Hydraulic Conductivity (cm/s)	0.044
Logger installation depth (meters from top of the well casing)	10
Well vertical profile (shallow) (m)	(0.0–9.0): sand; (9.0–12.4): gravel
Soil type	Entisols—Fluvents
Slope around the site	0–2%



**Fig. 2.** Time-series plot of the observed rainfall and groundwater level values.

**Table 2**  
Statistical parameters of the used data set.

Data period	Data set	Statistical parameters					
		$X_{mean}$	$X_{max}$	$X_{min}$	$S_X$	$C_V$	$C_{SX}$
Training period	$P$ (mm)	4.6	255	0	17.7	3.9	7.2
	$h$ (m)	119.6	123.6	119.1	0.43	0.003	3.3
	$ET$ (mm)	2.54	6.41	0.24	1.64	0.64	0.24
Testing period	$P$ (mm)	3.3	177	0	12.1	3.6	7.1
	$h$ (m)	119.4	122.4	119.1	0.36	0.003	3.1
	$ET$ (mm)	2.58	6.58	0.32	1.66	0.65	0.26
Whole period	$P$ (mm)	4.25	256	0	16.5	3.9	7.4
	$h$ (m)	119.5	123.6	119.1	0.42	0.003	3.2
	$ET$ (mm)	2.55	6.58	0.24	1.65	0.65	0.24

July 2006 when the highest amount of the seasonal rainfall has been occurred. Table 2 represents the statistical parameters of the used data, where  $X_{mean}$ ,  $X_{max}$ ,  $X_{min}$ ,  $S_X$ ,  $C_V$  and  $C_{SX}$  denote the mean, maximum, minimum, standard deviation, coefficient of variation and skewness, respectively. From the table it is observed that the rainfall data have much more skewed distribution than groundwater level data. In the mathematical sciences, a stationary process is a stochastic process whose joint probability distribution does not change when shifted in time or space. Consequently, parameters such as the mean and variance, if they exist, also do not change over time or position. Therefore, based on the statistics presented in Table 2, it may be concluded that the data used for training, testing and validation are stationary. Then, logically, the ARMA method was used [instead of ARIMA (Auto Regressive Integrated Moving Average) which is suitable for non stationary data], for comparisons. Nevertheless, there is a low non-stationarity in the applied data (as SD of test period is a bit different from train and validation periods). Therefore, it is expected that the difference between ARMA and ARIMA is not significant. In this study, several input combinations are tried

using the applied models to forecast 1-day and 7-day ahead groundwater level fluctuations. The input variables consist of the previously recorded groundwater levels ( $h_t$ ,  $h_{t-1}$  and  $h_{t-2}$ ) as well as precipitation values ( $P_{t-4}$ ,  $P_{t-3}$ ,  $P_{t-2}$ ,  $P_{t-1}$ ,  $P_t$ ) and the forecasted output variable is the groundwater level at times  $t+1$  and  $t+7$  (i.e.  $h_{t+1}$  and  $h_{t+7}$ ). The numbers of lags for groundwater level values are selected according to the partial auto-correlation function (PACF) of daily groundwater level data (Fig. 3). It is clear from this figure that the first three lags have significant effect on  $h_{t+1}$ . In order to determine the number of rainfall values that have a significant influence on forecasted groundwater level, the cross-correlation statistics of the rainfall-groundwater level data are applied with employing Coefficient of Determination ( $R^2$ ) criteria. The cross-correlation plot is also given in Fig. 3. In this figure the  $R^2$  statistics of cross-correlation is plotted along with the increasing rate of  $R^2$  (with lag time), according to the procedure suggested by Sudher et al. (2002). From the statistics of this figure it is found that the rainfall data up to 4 lags are able to explain 66% ( $R^2$  explainability) of the total variance, so it is decided to introduce rainfall values as models inputs up to 4 lags.

## 2.2. Gene expression programming (GEP)

Genetic programming (GP), proposed by Koza (1992), as a generalization of Genetic Algorithm (GA) (Goldberg, 1989), employs a “parse tree” structure for the search of its solutions. This technique has the capability for deriving a set of explicit formulations that rule the phenomenon, to describe the relationship between the independent and dependent variables using various operators.

According to Ferreira (2001b), the advantages of a system like GEP are clear from nature, but the most important are (i) the chromosomes are simple entities: linear, compact, relatively small, easy to manipulate genetically (replicate, mutate, recombine, etc); (ii) the expression trees are exclusively the expression of their respective chromosomes; they are entities upon which selection acts, and according to fitness, they are selected to reproduce with modification. Fig. 4 illustrates a schematic representation of GEP modeling procedure. In the present study the GeneXpro program (Ferreira 2001a) is used for modeling groundwater table fluctuations.

The procedure for predicting groundwater table fluctuations is as follows. The first step is the fitness function. For this problem, the Root Relative Squared Error (RRSE) is employed as advised by Shiri and Kisi (2011a). The Root Mean Squared Error (RMSE) fitness function,  $E_i$  of an individual program,  $i$ , is defined as (Ferreira, 2006):

$$E_i = \sqrt{\frac{1}{n} \sum_{j=1}^n (P_{ij} - T_j)^2} \quad (1)$$

where  $P_{ij}$  is the simulated value of the individual program  $i$  for fitness case  $j$  (out of sample case), and  $T_j$  is the target value for

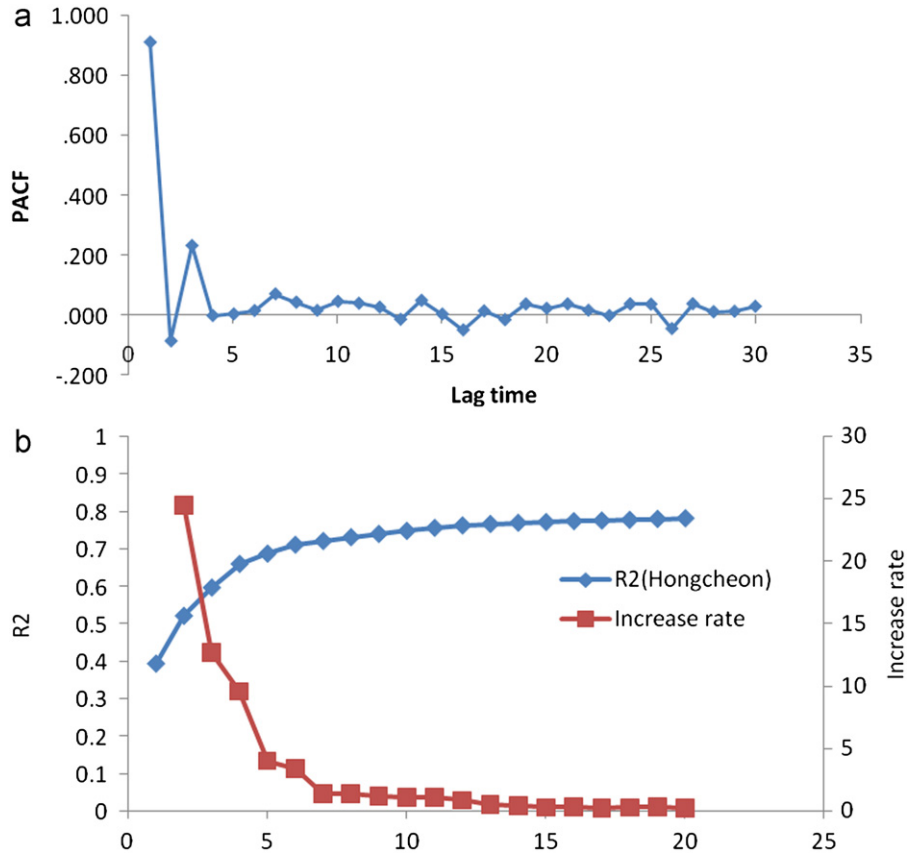


Fig. 3. (a) Partial auto correlation function of groundwater level data (b) Cross-correlation plot of the precipitation-groundwater level time series.

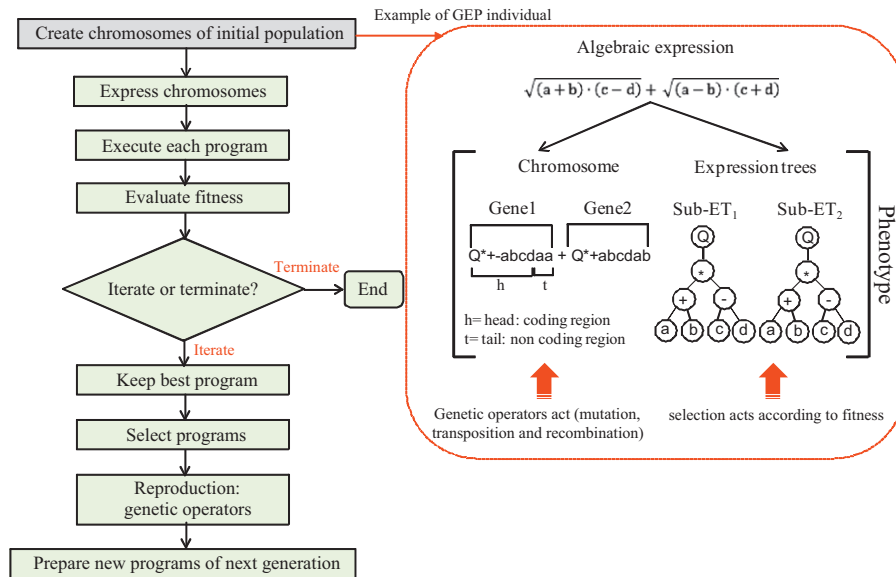


Fig. 4. Schematic representation of GEP modeling procedure.

fitness case  $j$ . For a perfect fit,  $P_{ij} = T_j$  and  $E_i = 0$ . For evaluating the fitness  $f_i$  of an individual program  $i$ , the following equation is applied:

$$f_i = 1000 \frac{1}{1 + E_i} \quad (2)$$

which obviously ranges between 0 and 1000 with 1000 corresponded to the ideal (Ferreira, 2006). In case of the application of

Parsimony Pressure for penalizing the parse tree, which uses the fitness measure as raw fitness, the raw maximum fitness is  $rf_{max} = 1000$ , and the overall fitness  $f_{ppi}$  (with parsimony pressure) is evaluated by:

$$f_{ppi} = rf_i \cdot \left[ 1 + \frac{1}{5000} \cdot \frac{S_{max} - S_i}{S_{max} - S_{min}} \right] \quad (3)$$



where the  $S_i$  is the program size,  $S_{max}$  and  $S_{min}$  are the maximum and minimum program sizes, respectively and are evaluated by:

$$S_{max} = G(h + t) \quad (4)$$

$$S_{min} = G \quad (5)$$

where  $G$  is the number of genes and  $h$  and  $t$  are, respectively, the head and tail sizes. In this case the  $f_{ppmax}$  is evaluated by the following formula:

$$f_{ppmax} = 1.0002rf_{max} \quad (6)$$

The second step consists of choosing a set of terminals  $T$  and a set of functions  $F$ , to create the chromosomes. In the current problem, the terminal set includes groundwater table height values ( $h_i$ ) as well as the corresponding simultaneous precipitation values ( $P_i$ ),  $i$  denotes the  $i$ th time step. The choice of the appropriate function is also based on discussions of Shiri and Kisi (2011a), so basic arithmetic operators ( $+$ ,  $-$ ,  $*$ ,  $/$ ) as well as some of the other basic mathematical functions ( $\sqrt{\phantom{x}}$ ,  $\sqrt[3]{\phantom{x}}$ ,  $\ln(x)$ ,  $e^x$ ,  $x^2$ ,  $x^3$ ) are applied. The third step is to choose the chromosomal architecture. Length of head,  $h=8$ , and three genes per chromosomes have been employed, which are commonly used values in the literature (e.g., Ferreira 2001a, 2001b; Ferreira, 2006). The fourth step is to choose the linking function. The linking function must be chosen as “addition” or “multiplication” for algebraic sub trees (Ferreira 2001a). Here, the sub trees are linked by addition. The fifth and final step is to choose the genetic operators. The parameters used per run are summarized in Table 3. The values presented in Table 3 are the default values of GeneXpro which may be applied for modeling issues (e.g., Shiri and Kisi, 2011a).

### 2.3. Adaptive-neuro-fuzzy inference system (ANFIS)

ANFIS is a combination of an adaptive neural network and a fuzzy inference system (FIS). A FIS is composed of five sub-blocks as follows (Jang 1993): rule base (containing a number of IF-THEN rules), data base (which defines the membership functions of the used fuzzy sets), decision making unit (performs the inference operations on the rules), fuzzification interface (transforms the crisp inputs into degrees of match with linguistic values) and defuzzification interface (transforms the fuzzy results of the interface to crisp output). The adaptive neural network is a superset of all kinds of feed-forward neural networks (Jang 1993). The parameters of the FIS are determined by the NN learning algorithms. Since this system is based on the FIS, reflecting extensive knowledge, an important aspect is that the system should be always interpretable in terms of fuzzy IF-THEN rules. ANFIS is capable of approximating any real continuous function on a compact set (Jang et al., 1997). There are two approaches for FISs, namely the approach of Mamdani

(Mamdani and Assilian, 1975) and approach of Sugeno (Takagi and Sugeno, 1985). The difference between the two approaches arises from the consequent part where Mamdani's approach uses fuzzy membership functions, while linear or constant functions are used in Sugeno's approach. In this study the Sugeno method was applied for modeling groundwater level fluctuations because it is more compact and computationally efficient than a Mamdani system. On the other hand, Sugeno based ANFIS is successfully used in modeling nonlinear phenomena in the literature (e.g., sediment modeling, Kisi, 2005; Kisi et al., 2008; rainfall-runoff modeling, Vernieuwe et al., 2005; evaporation modeling, Moghaddamnia et al., 2009; groundwater level prediction, Shiri and Kisi, 2011).

As a simple example a fuzzy inference system with two inputs  $x$  and  $y$  and one output  $z$  is assumed. Here,  $x$  and  $y$  might be considered as groundwater table depth and rainfall amount,  $h_{t-1}$  and  $P_{t-1}$ , in  $t-1$  time step, while the output  $z$  would represent the water table depth at time  $t$  ( $h_t$ ). Suppose that the rule base contains two fuzzy IF-THEN rules:

$$\text{Rule1 : if } x \text{ is } A_1 \text{ and } y \text{ is } B_1, \text{ then } f_1 = p_1x + q_1y + r_1 \quad (7)$$

$$\text{Rule2 : if } x \text{ is } A_2 \text{ and } y \text{ is } B_2, \text{ then } f_2 = p_2x + q_2y + r_2 \quad (8)$$

The IF (antecedent) part is fuzzy in nature, while the THEN (consequent) part is a crisp function of an antecedent variable (as a rule, a linear equation). The study presented here for ground water table, for the above example Eqs. (7) and (8) can be written as:

Rule 1: IF  $h_{t-1}$  is LOW and  $P_{t-1}$  is MEDIUM, THEN

$$h_t = p_1 h_{t-1} + q_1 P_{t-1} + r_1$$

Rule 2: IF  $h_{t-1}$  is LOW and  $P_{t-1}$  is HIGH, THEN

$$h_t = p_2 h_{t-1} + q_2 P_{t-1} + r_2 \dots$$

where  $p_i$ ,  $q_i$  and  $r_i$  are parameters with  $i=1, 2, 3, \dots, n$  corresponding to Rule 1, Rule 2, Rule 3, ..., Rule  $n$ . The corresponding equivalent ANFIS architecture is represented in Fig. 5. The node function in the same layer of the same function family is described as follow (Jang, 1993):

Layer 1: Every node  $i$  in this layer is an adaptive node with node function

$$O_i^1 = \mu_{A_i}(h_{t-1}) \quad (9)$$

where  $h_{t-1}$  is the input to the  $i$ th node and  $A_i$  is a linguistic label (such as HIGH, LOW or MEDIUM) associated with this node function. A similar equation as Eq. (9) may be considered for the input  $P_{t-1}$ .

**Table 3**  
General description of the applied GEP models.

Number of chromosomes	30	One point recombination rate	0.3
Head size	8	Two point recombination rate	0.3
Number of genes	3	Gene recombination rate	0.1
Linking function	addition	Gene transposition rate	0.1
Fitness function error type	RRSE	Insertion sequence transposition rate	0.1
Mutation rate	0.044	Root insertion sequence transposition	0.1
Inversion rate	0.1	Penalizing tool	Parsimony Pressure
Mutation	Allows the evolution of good solutions for the studied models to virtually all problems		
Inversion	Inversion is restricted to the heads of genes		
One-point recombination	The parent chromosomes are paired and split up at exactly the same point		
Two-point recombination	Two parent chromosomes are paired and two points are randomly chosen as crossover points		
Gene recombination	Entire genes are exchanged between two parent chromosomes, forming two daughter chromosomes containing genes from both parents		
Gene transposition	An entire gene works as a transposon and transposes itself to the beginning of the chromosome		
IS transposition	Short fragments of the genome with a function or terminal in the first position that transpose to the heads of gene except the root		
RIS transposition	Short fragments with a function in the first position that transpose to the start position of genes		

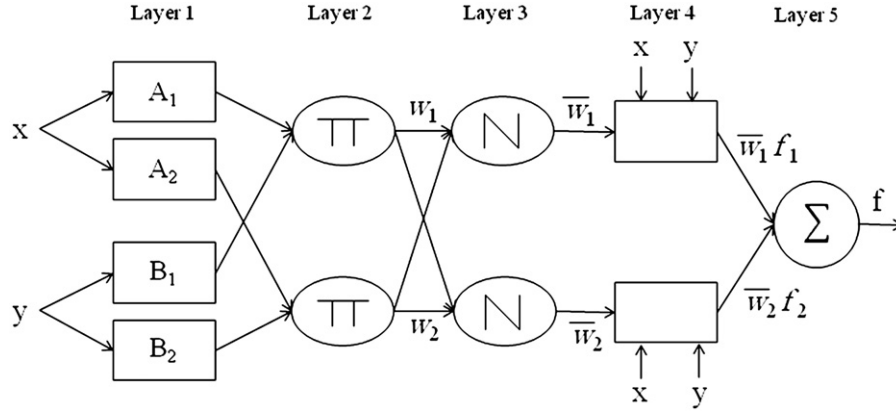


Fig. 5. Schematic ANFIS procedure.

The node function  $O_i^1$  is the membership function of  $A_i$  and specifies the degree to which the given input  $h_{t-1}$  (or  $P_{t-1}$ ) satisfies the quantifier  $A_i$ . The membership function for  $A$  is usually described by bell-functions,

$$A_i(h_{t-1}) = \frac{1}{1 + [(h_{t-1} - c_i)/a_i]^{2b_i}} \quad (10)$$

where  $\{a_i, b_i, c_i\}$  is the parameter set and  $\mu$  is the membership function of  $A_i$ . As the values of these parameters change, the bell-shaped function varies accordingly, thus exhibiting various forms of membership functions depending on the linguistic label  $A_i$ . In fact, any continuous and piecewise differentiable functions, such as commonly used triangular or trapezoidal membership functions, are also qualified candidates for node function in this layer. Parameters in this layer are referred to as *premise parameters*.

Layer 2: This layer consists of circle nodes labeled TT which multiply incoming signals and sending the product out. For instance

$$O_i^2 = w_i = A_i(h_{t-1}) B_i(P_{t-1}), \quad i = 1, 2. \quad (11)$$

Each node output represents the firing strength of a rule.

Layer 3: In this layer, the circle nodes labeled N, calculate the ratio of the  $i$ th rule firing strength to the sum of all rule firing strengths

$$O_i^3 = \bar{w}_i = \frac{w_i}{w_1 + w_2}, \quad \text{for } i = 1, 2. \quad (12)$$

The outputs of this layer are referred to as *normalized firing strengths*.

Layer 4: All of the nodes in this layer are adaptive with a node function

$$O_i^4 = \bar{w}_i f_i = \bar{w}_i(p_i h_{t-1} + q_i P_{t-1} + r_i) \quad (13)$$

where  $\bar{w}_i$  is the output of layer 3, and  $\{p_i, q_i, r_i\}$  is the parameter set. Parameters in this layer are called *consequence parameters*. Layer 5: The single circle node of this layer, labeled  $\Sigma$ , computes the overall outputs as the summation of all incoming signals:

$$O_i^5 = \frac{\sum_i \bar{w}_i f_i}{\sum_i \bar{w}_i} \quad (14)$$

In implementation of fuzzy logic, several types of MFs can be used. However, recent studies have shown that, the type of MF does not affect the results fundamentally (Vernieuwe et al., 2005). In the present study, the triangular MFs are used. The number of MFs has been determined iteratively. In the present

study a program was written in MATLAB to establish the ANFIS models. Detailed information about ANFIS may be found in e.g. Jang (1993).

#### 2.4. Artificial neural networks (ANNs)

The ANN is a computing framework patterned after the behavior of biological neural networks. In this study, a multilayer perceptron network (MLPN) with one hidden layer trained by the back-propagation algorithm (BPA) (Rumelhart and McClelland, 1986) was employed to build the ANN models, which has been most commonly used ANN configuration (Maier and Dandy, 2000; Maier et al., 2010). The mathematical expression of the MLPN feed-forwarding process is as follows:

$$y_n = f\left(\sum_{m=1}^L w_{nm} x_m + b_n\right) \quad (15)$$

where  $m$  and  $n$  denote nodes in the previous and present layer, respectively,  $x$  and  $y$  denote nodal values in the previous and present layer, respectively,  $w$  is a weight value between  $x$  and  $y$ ,  $b$  is a bias in the present layer,  $L$  is the number of nodes in the previous layer, and  $f$  is an activation function such as a log sigmoid function employed in the present study. The weight updating rule of the ANN training process by BPA are described as follows:

$$w^{i+1} - w^i = \beta (w^i - w^{i-1}) + (1 - \beta) \alpha \left( -\frac{\partial E^i}{\partial w^i} \right) \quad (16)$$

Where  $i$  denotes  $i$ th iteration,  $\alpha$  is a learning rate,  $\beta$  is a momentum value,  $E$  is the summation of squared errors between observed and estimated values.

In order to calibrate the model parameters, which are the number of hidden nodes, the learning rate and the momentum value, the data set of the training period is divided into two parts of training and calibration sets. The stopping criteria of the model building were set to terminate the training process when the error of the calibration stage begins to increase. The model parameters were selected by trial and error approach and one hundred sets of random initial weights were considered to avoid the ANN model being captured in a local minimum. All the model building process was implemented by C language.

#### 2.5. Support vector machine (SVM)

The SVM has become a relatively novel and promising estimator in data-driven research fields, of which basic concept and theory

have been introduced by Vapnik (1995, 1998). The generalization ability of the SVM is considered to be better than ANN, in the sense that it is based on the structural risk minimization rather than the empirical risk minimization of the ANN. The main process of SVM model building consists of selecting support vectors which support the model structure and determining their weights. The process of an SVM estimator ( $f$ ) on regression can be described as:

$$f(\mathbf{x}) = \mathbf{w} \varphi(\mathbf{x}) + b \quad (17)$$

where  $\mathbf{w}$  is a weight vector, and  $b$  is a bias, and  $\varphi$  is a nonlinear transfer function mapping the input space into a high-dimensional feature space. Vapnik (1995) introduced an object function of convex optimization with  $\varepsilon$ -insensitivity loss function for solving the Eq. (3), of which mathematical expressions are described as

$$\begin{aligned} &\underset{\mathbf{w}, b, \xi, \xi^*}{\text{minimize}} \quad \frac{1}{2} \|\mathbf{w}\|^2 + C \sum_{k=1}^N (\xi_k + \xi_k^*) \\ &\text{subject to} \quad \begin{cases} y_k - \mathbf{w}^T \varphi(\mathbf{x}_k) - b \leq \varepsilon + \xi_k \\ \mathbf{w}^T \varphi(\mathbf{x}_k) + b - y_k \leq \varepsilon + \xi_k^* \\ \xi_k, \xi_k^* \geq 0 \end{cases} \quad k = 1, 2, \dots, N \end{aligned} \quad (18)$$

where  $\xi$  and  $\xi^*$  are slack variables penalizing estimation error by the  $\varepsilon$ -insensitivity loss function, and  $C$  is a positive tradeoff parameter for the degree of the empirical error. In the present research, in order to solve this optimization problem the sequential minimal optimization (SMO) algorithm, introduced by Platt (1999) and Schölkopf and Smola (2002) has been employed.

The object function of Eq. (18) can be reformulated using Lagrangian multipliers of  $(\alpha, \alpha^*)$ , as described below,

$$\begin{aligned} &\underset{\alpha, \alpha^*}{\text{maximize}} \quad \begin{cases} -\frac{1}{2} \sum_{k,l=1}^N (\alpha_k - \alpha_k^*)(\alpha_l - \alpha_l^*) K(\mathbf{x}_k, \mathbf{x}_l) \\ -\varepsilon \sum_{k=1}^N (\alpha_k + \alpha_k^*) + \sum_{k=1}^N y_k (\alpha_k - \alpha_k^*) \end{cases} \\ &\text{subject to} \quad \begin{cases} \sum_{k=1}^N (\alpha_k - \alpha_k^*) = 0 \\ 0 \leq \alpha_k, \alpha_k^* \leq C \end{cases} \end{aligned}$$

$$\text{to obtain} \quad f(\mathbf{x}) = \sum_{k=1}^n (\alpha_k - \alpha_k^*) K(\mathbf{x}, \mathbf{x}_k) + b \quad (18-1)$$

where  $K$  is a kernel function and  $n$  is the number of support vectors. In this study, a radial basis kernel function with parameter  $\sigma$  was used, which is expressed as

$$K(\mathbf{x}_k, \mathbf{x}_l) = \exp\left(-\frac{\|\mathbf{x}_k - \mathbf{x}_l\|^2}{2\sigma^2}\right) \quad (18-2)$$

The model parameters of the SVM trained by SMO are  $C$ ,  $\varepsilon$ , and  $\sigma$ . The model parameter selection rule and the stopping criteria were the same as the ANN.

The computer code for SVM was developed using C language. Fig. 6 shows the ANN & SVM models schematic representations.

### 3. Analysis of the results

The trained and tested models of the data specified for the selected site were used to forecast groundwater levels over the next and up to 7 days beyond the data records. Four statistical evaluation parameters were used to assess the models' performances:

#### 1. Correlation Coefficient ( $R$ )

$$R = \frac{\sum_{i=1}^n (h_o - \bar{h}_o)(h_M - \bar{h}_M)}{\sqrt{\sum_{i=1}^n (h_o - \bar{h}_o)^2 \sum_{i=1}^n (h_M - \bar{h}_M)^2}} \quad (19)$$

#### 2. Root Mean Squared Error (RMSE)

$$\text{RMSE} = \sqrt{\frac{1}{n} \sum_{i=1}^n (h_M - h_o)^2} \quad (20)$$

#### 3. Ratio of standard deviation of predicted to observed values (CO)

$$\text{CO} = \sqrt{\frac{\sum_{i=1}^n (h_M - \bar{h}_M)^2}{\sum_{i=1}^n (h_o - \bar{h}_o)^2}} \quad (21)$$

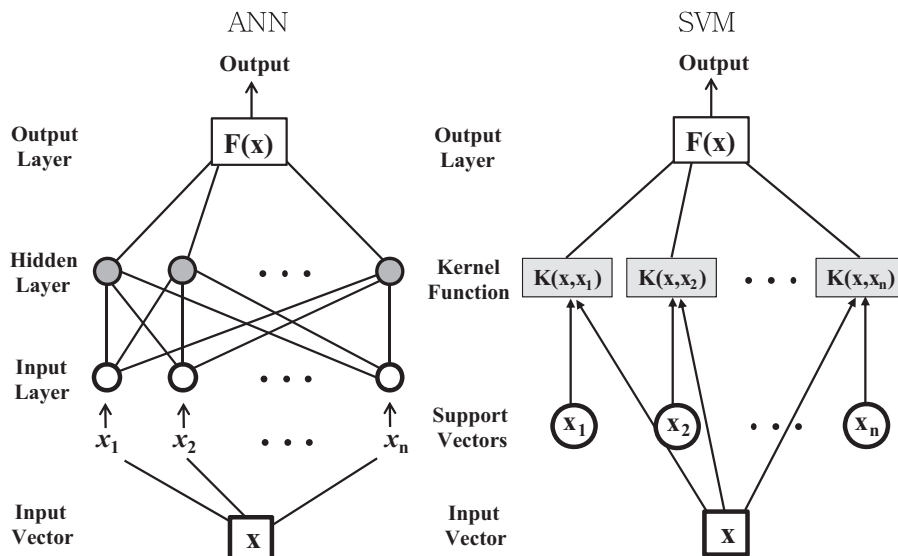


Fig. 6. ANN & SVM models schematic representation.

#### 4. Nash-Sutcliffe Coefficient (NS)

$$NS = \left[ 1 - \frac{\sum_{i=1}^n (h_M - h_o)^2}{\sum_{i=1}^n (h_o - \bar{h}_o)^2} \right] * 100 \quad (22)$$

Where  $h_o$  is the groundwater level observed at the  $i$ th time step,  $h_M$  is the corresponding simulated value,  $n$  is the number of time steps,  $\bar{h}_o$  is the mean of observational values and  $\bar{h}_M$  is the mean value of the simulations.  $R$  ranges between 0 and 1, and its higher values indicating better performance of a model. According to Legates and McCabe (1999) the Pierson correlation coefficient ( $R$ ) alone should not be employed to evaluate the goodness-of-fit of model simulations because of the standardization inherent of this coefficient as well as its sensitivity to outliers. Therefore, it is advisable to quantify the error in the same unit as for the variables (i.e., RMSE) along with the application of correlation coefficients. RMSE describes the average magnitude of the errors by attributing more weight to large errors and ranges between 0 and  $\infty$  with lower values corresponding to better model performance. CO parameter also represents a better model if its value approaches 1. Also the Nash-Sutcliffe coefficient (NS) can provide good insight about the applied model. The optimal value of NS is 1, representing the perfect fit.

#### 4. Results and discussions

This study aims at application of various AI models viz., GEP, ANFIS, ANN and SVM to forecast groundwater level up to seven days beyond data records. In the first part of the study, the applied models were examined by various input combinations of groundwater level ( $h$ ), precipitation ( $P$ ) and evapotranspiration

**Table 4**  
Testing statistics of the groundwater level-based models.

Input variables	$R$	RMSE ( $m$ )	CO
<b>GEP</b>			
$h_t$	0.934	0.132	0.996
$h_{t-1}$ and $h_t$	0.958	0.105	0.998
$h_{t-2}$ , $h_{t-1}$ and $h_t$	0.967	0.093	1.002
<b>ANFIS</b>			
$h_t$	0.942	0.123	0.964
$h_{t-1}$ and $h_t$	0.950	0.115	0.994
$h_{t-2}$ , $h_{t-1}$ and $h_t$	0.958	0.104	0.973
<b>ANN</b>			
$h_t$	0.936	0.128	0.926
$h_{t-1}$ and $h_t$	0.928	0.135	0.941
$h_{t-2}$ , $h_{t-1}$ and $h_t$	0.944	0.119	0.941
<b>SVM</b>			
$h_t$	0.940	0.125	0.982
$h_{t-1}$ and $h_t$	0.942	0.123	0.924
$h_{t-2}$ , $h_{t-1}$ and $h_t$	0.935	0.129	0.917
<b>ARMA</b>			
ARMA(1,0)	0.966	0.133	1.000
ARMA(2,0)	0.967	0.131	1.007
ARMA(3,0)	0.971	0.124	0.989
ARMA(4,0)	0.971	0.124	0.990
ARMA(1,1)	0.967	0.131	1.006
ARMA(2,1)	0.967	0.131	1.001
ARMA(1,2)	0.969	0.128	1.000
ARMA(2,2)	0.966	0.132	1.001
ARMA(3,1)	0.971	0.124	0.990
ARMA(1,3)	0.969	0.127	1.001
ARMA(3,2)	0.970	0.124	0.990
ARMA(2,3)	0.967	0.130	1.000
ARMA (3,3)	0.970	0.124	0.988

(ET) data to forecast  $h_{t+1}$ . Once the best model structure and corresponding input combination was selected, it will be used to forecast 7-day fluctuations. It should be remarked that there were three groups of input combinations in the present application, which (1) groundwater level based ( $h$ -based): employs the groundwater level data to forecast  $h_{t+1}$ , (2) precipitation based ( $P$ -based): employs the precipitation data to forecast  $h_{t+1}$ , and (3) evapotranspiration based ( $ET$ -based): employs the ET data to forecast  $h_{t+1}$ . Subsequently, the optimal input combinations of each data group would then be merged to improve the models' accuracy. In order to assess the applied models to traditional techniques, the Auto-Regressive Moving Average (ARMA) technique was applied for making comparison with groundwater level based models.

**Table 5**  
Testing statistics of the precipitation-and ET-based models.

Input variables	$R$	RMSE ( $m$ )	CO
<b>Precipitation-based models</b>			
<b>GEP</b>			
$P_t$	0.560	0.352	0.534
$P_{t-1}$ and $P_t$	0.712	0.305	0.562
$P_{t-2}$ , $P_{t-1}$ and $P_t$	0.648	0.327	0.646
$P_{t-3}$ , $P_{t-2}$ , $P_{t-1}$ and $P_t$	0.756	0.278	0.765
$P_{t-4}$ , $P_{t-3}$ , $P_{t-2}$ , $P_{t-1}$ and $P_t$	0.795	0.284	0.899
<b>ANFIS</b>			
$P_t$	0.641	0.338	0.523
$P_{t-1}$ and $P_t$	0.737	0.302	0.626
$P_{t-2}$ , $P_{t-1}$ and $P_t$	0.791	0.265	0.673
$P_{t-3}$ , $P_{t-2}$ , $P_{t-1}$ and $P_t$	0.826	0.261	0.672
$P_{t-4}$ , $P_{t-3}$ , $P_{t-2}$ , $P_{t-1}$ and $P_t$	0.849	0.248	0.706
<b>ANN</b>			
$P_t$	0.594	0.317	0.532
$P_{t-1}$ and $P_t$	0.715	0.290	0.594
$P_{t-2}$ , $P_{t-1}$ and $P_t$	0.772	0.279	0.589
$P_{t-3}$ , $P_{t-2}$ , $P_{t-1}$ and $P_t$	0.819	0.263	0.649
$P_{t-4}$ , $P_{t-3}$ , $P_{t-2}$ , $P_{t-1}$ and $P_t$	0.818	0.270	0.559
<b>SVM</b>			
$P_t$	0.595	0.304	0.391
$P_{t-1}$ and $P_t$	0.715	0.274	0.460
$P_{t-2}$ , $P_{t-1}$ and $P_t$	0.758	0.250	0.649
$P_{t-3}$ , $P_{t-2}$ , $P_{t-1}$ and $P_t$	0.809	0.236	0.595
$P_{t-4}$ , $P_{t-3}$ , $P_{t-2}$ , $P_{t-1}$ and $P_t$	0.841	0.213	0.670
<b>ET-based models</b>			
<b>GEP</b>	0.585	0.344	0.556
<b>ANFIS</b>	0.342	0.351	0.586
<b>ANN</b>	0.586	0.325	0.651
<b>SVM</b>	0.585	0.323	0.778

**Table 6**  
Testing statistics of the applied models using the merged input combinations (1-day ahead forecast interval).

Applied model	$R$	RMSE( $m$ )	CO	NS
<b>GW+P</b>				
GEP	0.981	0.071	1.03	96.1
ANFIS	0.966	0.099	1.060	92.6
ANN	0.963	0.111	0.886	90.6
SVM	0.977	0.077	1.001	95.4
<b>GW+ET</b>				
GEP	0.945	0.119	0.955	89.4
ANFIS	0.912	0.110	0.991	89.2
ANN	0.949	0.115	0.973	90.1
SVM	0.934	0.132	0.988	87.1
<b>GW+P+ET</b>				
GEP	0.987	0.06	1.03	97.3
ANFIS	0.948	0.085	0.99	94.6
ANN	0.981	0.07	0.972	96.3
SVM	0.976	0.08	1.01	95.1



Table 4 summarizes the error statistics of groundwater level based models during the test period. From the table it can be obtained that GEP model gives the best results among other applied models with relatively low error and high correlation values. Although the  $R$  values of ARMA models are generally higher than those of GEP, this term provides information for linear dependence between observations and corresponding simulations and even though a  $R$  value equal to 1 does not guarantee that a model captures the behavior of the investigated

time series (Kisi et al., 2008). The table clearly represents that the triple-groundwater level-input to GEP model is superior to single- and double-groundwater level-input models and this is in complete agreement with PACF analysis.

Testing results of the applied  $P$ -based and  $ET$ -based models are listed in Table 5 in terms of  $R$ , RMSE and CO. Similar to groundwater level-based models; GEP surpasses all the other applied models in forecasting  $h_{t+1}$  with relatively low errors. In order to increase the models' accuracy the optimal groundwater level-

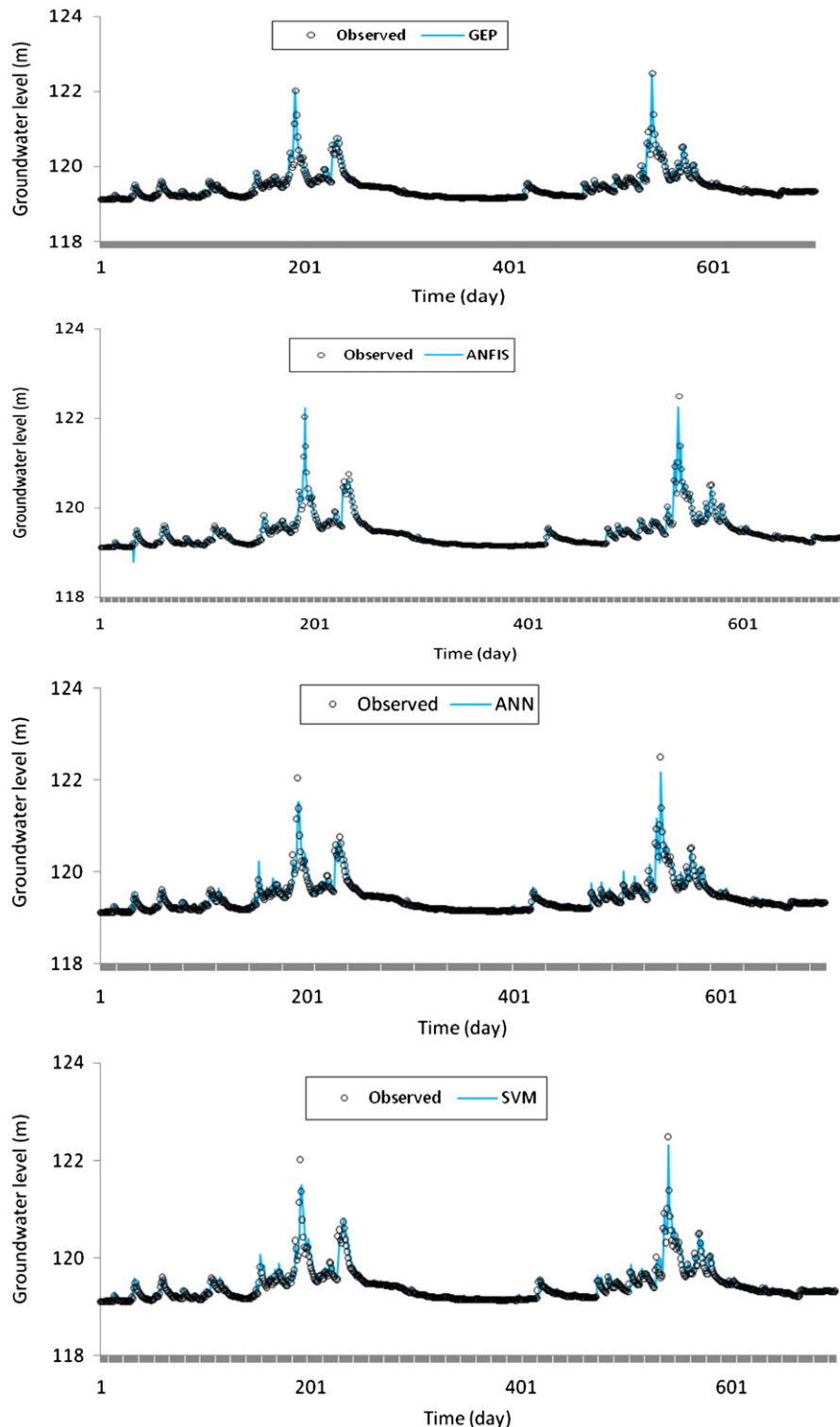


Fig. 7. Observed and forecasted  $h_{t+1}$  values using applied models during the test period.

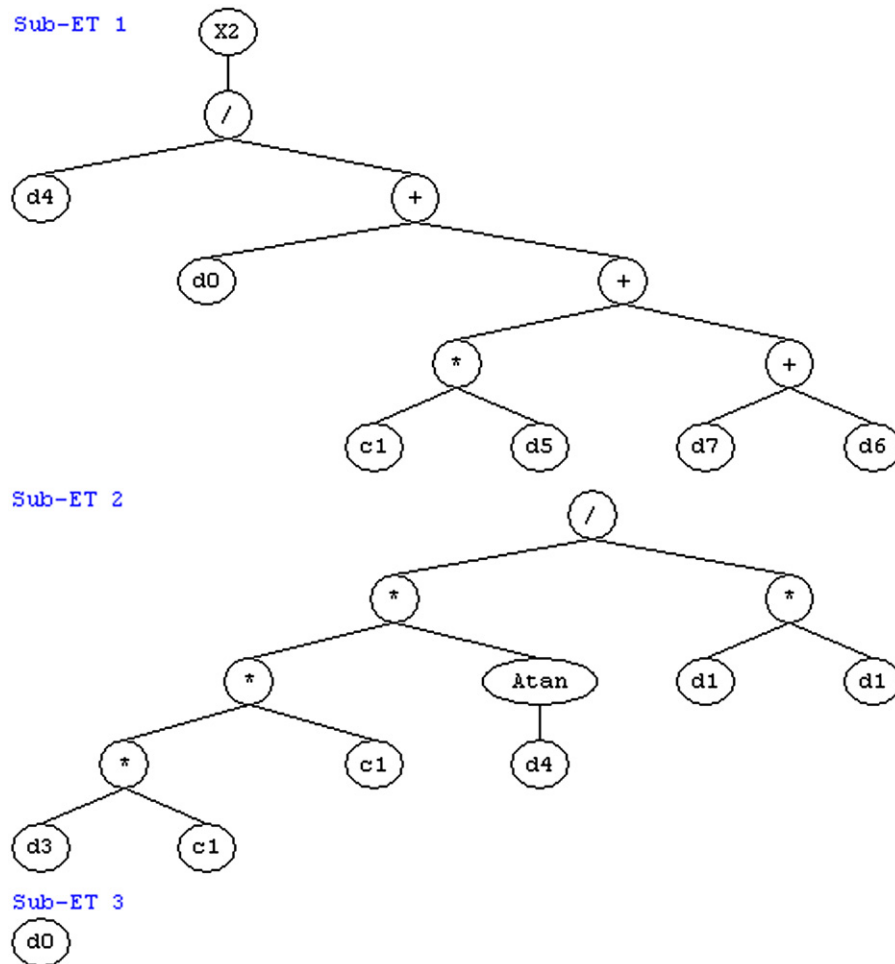


Fig. 8. Expression tree of GEP model for 1-day ahead prediction (using new input combination).

Table 7

Testing statistics of the applied models using the merged input combinations (7-day ahead forecast interval).

Applied model	R	RMSE(m)	CO	NS
<b>GW+P</b>				
GEP	0.757	0.244	0.873	55.7
ANFIS	0.688	0.270	0.818	45.7
ANN	0.670	0.273	0.753	44.2
SVM	0.694	0.264	0.704	47.8
<b>GW+ET</b>				
GEP	0.718	0.264	0.876	48.2
ANFIS	0.703	0.272	0.858	45.2
ANN	0.705	0.265	0.781	47.9
SVM	0.688	0.279	0.664	42.3
<b>GW+P+ET</b>				
GEP	0.850	0.204	1.01	69.1
ANFIS	0.551	0.354	1.023	43.8
ANN	0.720	0.260	0.783	49.8
SVM	0.701	0.269	0.756	46.4

based, rainfall-based and ET-based input combinations were merged and the capabilities of the applied AI models were examined through using the new input combinations. Table 6 represents the statistical analysis of the results by using new input combinations. The table clearly shows that the GEP model is the best model among the applied models. The SVM model can be ranked as the second model. Fig. 7 displays the observed and forecasted groundwater levels by using various models during the test period. This figure shows that GEP model surpasses the other

applied models in forecasting daily groundwater level in 1-day and the SVM model is ranked as the second model. In these cases, the fit line in the scatterplots indicate that the slope and intercept for the GEP model are, respectively closer to 1 and 0 than those of the ANFIS, ANN and SVM models, exhibiting the high capability of GEP in modeling groundwater level fluctuations. Nonetheless, one of the main advantages of the GP (i.e., GEP) model over the other AI models (e.g. ANFIS, ANN and SVM) is the capability of GP in giving mathematical expressions for the studied phenomenon. Fig. 8 illustrates the expression tree of the GEP model (using new input combination) for 1-day water table forecast

$$h_{t+1} = h_t + \frac{47.61R_t \arctg(R_{t-1})}{h_{t-1}^2} + \frac{R_{t-1}}{h_t + 2.61R_{t-2} + R_{t-3} + ET} \quad (23)$$

In the second part of the study, the AI models capabilities for predicting 7-day forecast were investigated by using the optimal input combination, introduced in the previous part. Table 7 represents the statistical analysis of this forecast interval. Here also the GEP model performs better than the ANFIS, ANN and SVM models from the R, RMSE, CO and NS viewpoints. The 7-day forecast of each model is demonstrated in Fig. 9 in the form of hydrograph and scatter plot. It is clearly seen from this figure that the GEP 7-day forecast is better than the other models. The underestimation of the peak values are clearly seen for the ANFIS, ANN and SVM models.

The results were also tested using t-test for verifying the significance of differences between the observed and predicted. Both tests were set at a 95% significant level. The statistics of the

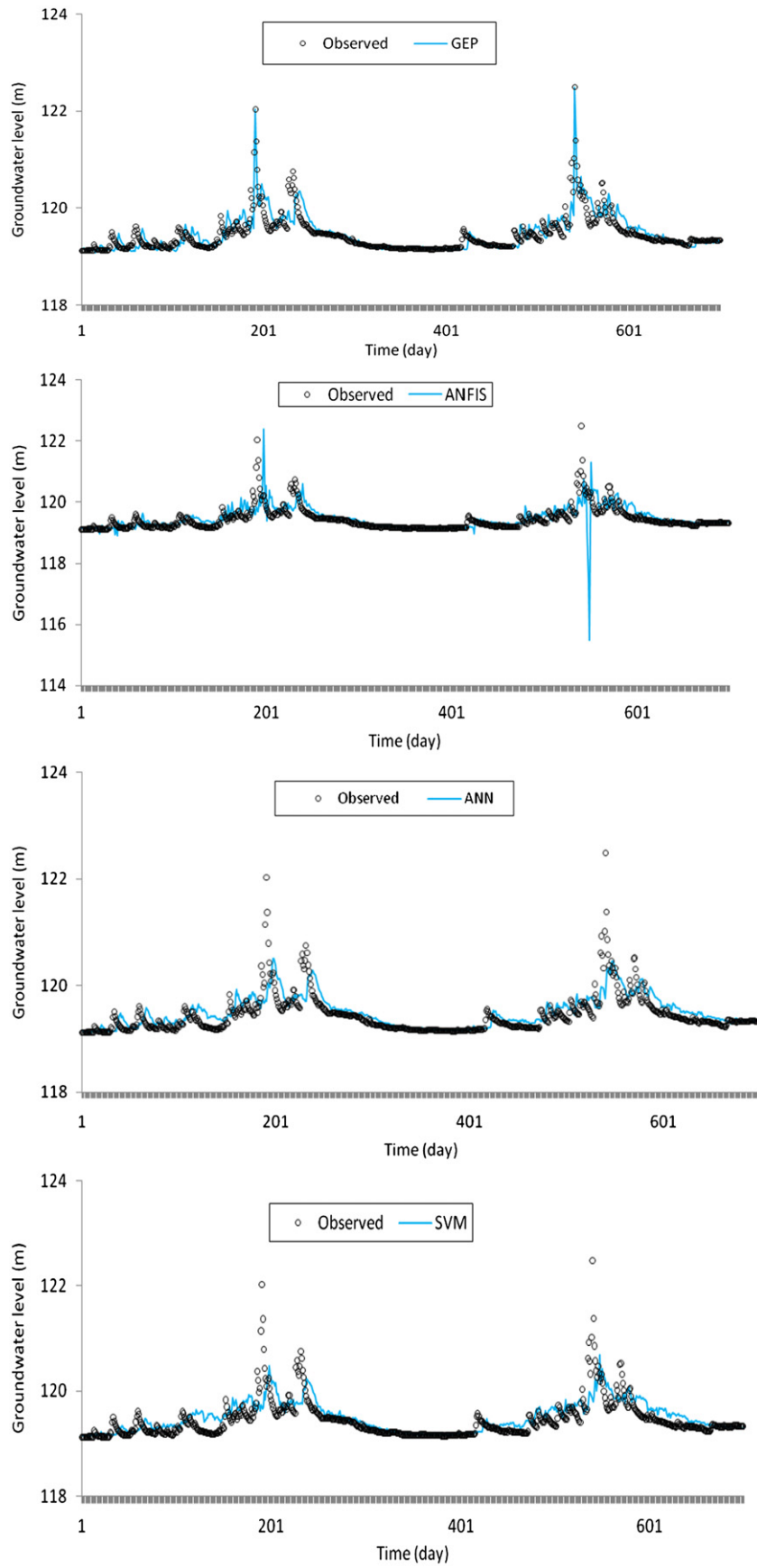


**Fig. 9.** Observed and forecasted  $h_{t+7}$  values using applied models during the test period.

**Table 8**  
t-test of the GEP, ANFIS, ANN and SVM models in estimating groundwater levels.

Method	1-day ahead forecast interval		7-day ahead forecast interval	
	t-Statistic	Resultant significance level	t-Statistic	Resultant significance level
GEP	0.126	0.900	1.502	0.133
ANFIS	0.086	0.932	0.352	0.725
ANN	0.420	0.675	2.701	0.007
SVM	0.786	0.432	1.374	0.170

tests are given in Table 8. The ANFIS and GEP models give small testing values with high significance levels for the 1-day ahead forecast. ANFIS seems to be slightly better than the GEP model. For the 7-day ahead forecast, the ANFIS model seems to be better than the other models. According to the t-test analysis, the SVM and ANN are the worst for estimating the 1- and 7-day forecast, respectively.

## 5. Conclusions

The accuracy of the Artificial Intelligence (AI) techniques, GEP, ANFIS and ANN, in forecasting short-term (one-day as well as 7-day) groundwater level (with rainfall and evapotranspiration effects implication) has been investigated in the present paper. In the first part of the study, the AI models were developed and tested employing different input combinations of daily groundwater level, rainfall and evapotranspiration data of Hongcheon well, operated by National Groundwater Monitoring Network (NGMN) of South Korea, and the results were compared with those of the ARMA model. Comparison results indicated that the AI models performed better than the ARMA technique. Among the AI methods, the GEP model outperformed the ANFIS, ANN and SVM models. It was found that the GEP model whose inputs were three previous groundwater level and four previous rainfall values had the best accuracy. In the second part of the study, the accuracy of AI models was compared with each other for 7-day period water table forecast. The optimal input combinations obtained in the first part of the study were used for each model. Comparison of the AI models indicated that the GEP model performed better than the ANFIS, ANN and SVM models. The present study used data from only one station and further studies using more data from various areas may be required to reinforce the conclusions drawn from this study.

## Acknowledgment

This research was partly supported by the Basic Research Project (12-3211) of the Korea Institute of Geo-science and Mineral Resources (KIGAM).

## References

Allen, R.G., Pereira, L.S., Raes, D., Smith, M., 1998. Crop evapotranspiration. Guide lines for computing crop evapotranspiration. FAO Irrigation and Drainage Paper no. 56, Rome, Italy.

Bierkens, M.F.P., 1998. Modeling water table fluctuations by means of a stochastic differential equation. *Water Resources Research* 34 (10), 2485–24499.

Box, G.E.P., Jenkins, G.M., 1976. Time series analysis: Forecasting and control. Holden Day, Boca Raton, Florida.

Coppola, E., Rana, A., Poulton, M., Szidarovszky, F., Uhl, V., 2005. A neural network model for predicting aquifer water level elevations. *Ground Water* 43 (2), 231–241.

Coppola, E., Szidarovszky, F., Davis, D., Spayad, S., Poulton, M., Roman, E., 2007. Multi objective analysis of a public wellfield using artificial neural networks. *Ground Water* 45 (1), 53–61.

Coulibaly, P., Anctil, F., Aravena, R., Bobee, B., 2001. Artificial neural network modeling of water table depth fluctuations. *Water Resources Research* 37 (4), 885–896.

Feng, S., Kang, S., Huo, Z., Chen, S., Mao, X., 2008. Neural networks to simulate regional groundwater levels affected by human activities. *Ground Water* 46 (1), 80–90.

Ferreira, C., 2001a. Gene expression programming in problem solving. In: Sixth Online World Conference on Soft Computing in Industrial Applications (invited tutorial).

Ferreira, C., 2001b. Gene expression programming: a new adaptive algorithm for solving problems. *Complex Systems* 13 (2), 87–129.

Ferreira, C., 2006. Gene Expression Programming: Mathematical Modeling by an Artificial Intelligence. Springer, Berlin, Heidelberg New York 478 pp.

Gill, M.K., Asefa, T., Kaheil, Y., McKee, M., 2007. Effect of missing data on performance of learning algorithms for hydrologic predictions: Implications to an imputation technique. *Water Resources Research* 43 (7), W07416.

Goldberg, D.E., 1989. Genetic algorithms in search, optimization, and machine learning. Addison-Wesley, Reading MA 432 pp.

Hipel, K.W., McLeod, A.I., 1994. Time series modeling of water resources and environmental systems. Development of Water Science, vol. 45. Elsevier Science, New York.

Hong, Y.S.T., White, P.A., 2009. Hydrological modeling using a dynamic neuro-fuzzy system with on-line and local learning algorithm. *Advances in Water Resources* 32, 110–119.

Jang, J.S.R., 1993. ANFIS: adaptive-network-based fuzzy inference system. *IEEE Transactions on Systems, Man and Cybernetics* 23 (3), 665–685.

Jang, J.S.R., Sun, C.T., Mizutani, E., 1997. Neurofuzzy and Soft Computing: a Computational Approach to Learning and Machine Intelligence. Prentice-Hall, New Jersey.

Khalil, A.F., McKee, M., Kemblowski, M., Asefa, T., Bastidas, L., 2006. Multiobjective analysis of chaotic dynamic systems with sparse learning machines. *Advances in Water Resources* 29, 72–88.

Kisi, O., 2005. Suspended sediment estimation using neuro-fuzzy and neural network approaches. *Hydrological Sciences Journal* 50 (4), 683–696.

Kisi, O., Yuksel, I., Dogan, E., 2008. Modelling daily suspended sediment of rivers in Turkey using several data driven techniques. *Hydrological Sciences Journal* 53 (6), 1270–1285.

Kisi, O., Shiri, J., 2012. Wavelet and neuro-fuzzy conjunction model for predicting water table depth fluctuations. *Hydrology Research* 43 (3), 286–300.

Koza, J.R., 1992. Genetic Programming: On the Programming of Computers by Means of Natural Selection, Cambridge, MA. The MIT Press 840 pp.

Legates, D.R., McCabe, G.J., 1999. Evaluating the use of goodness-of-fit measures in hydrologic and hydroclimatic model validation. *Water Resources Research* 35 (1), 233–241.

Maier, H.R., Dandy, G.C., 2000. Neural networks for the prediction and forecasting of water resources variables: a review of modeling issues and applications. *Environmental Modeling and Software* 15, 101–124.

Maier, H.R., Jain, A., Dandy, D.C., Sudheer, K.P., 2010. Methods used for the development of neural networks for the prediction of water resource variables in river system: current status and future directions. *Environmental Modeling and Software* 25, 891–909.

Mamdani, E.H., Assilian, S., 1975. An experiment in linguistic synthesis with a fuzzy logic controller. *International Journal of Man-Machine Studies* 7 (1), 1–13.

Moghaddamnia, A., Ghafari Gousheh, M., Piri, J., Amin, S., Han, D., 2009. Evaporation estimation using artificial neural networks and adaptive neuro-fuzzy inference system techniques. *Advances in Water Resources* 32, 88–97.

Nayak, P.C., Satyaji Rao, Y.R., Sudheer, K.P., 2006. Groundwater level forecasting in a shallow aquifer using artificial neural network approach. *Water Resources Management* 20, 77–90.

Platt, J.C., 1999. Fast training of support vector machines using sequential minimal optimization. In: Schölkopf, B., Burges, C.J.C., Smolar, A.J. (Eds.), *Advances in Kernel Methods—Support Vector Learning*. MIT Press, Cambridge, Massachusetts, USA.

Raghuathan, H.M., 2003. Ground Water, 2nd ed. New Age International Publishers, New Delhi 563.

Rizzo, D.M., Dougherty, D.E., 1994. Characterization of aquifer properties using artificial neural networks: neural Kriging. *Water Resources Research* 30 (2), 483–497.

Rumelhart, D.E., McClelland, J.L., 1986. Parallel Distributed Processing: Explorations in the Microstructure of Cognition. MIT Press, Cambridge, Massachusetts, USA, The PDP Research Group.



- Schölkopf, B., Smola, A.J., 2002. *Learning with Kernels: Support Vector Machines, Regularization, Optimization, and Beyond*. MIT Press, Cambridge, Massachusetts, USA.
- Shiri, J., Kisi, O., 2011. Comparison of genetic programming with neuro-fuzzy systems for predicting short-term water table depth fluctuations. *Computers & Geosciences* 37 (10), 1692–1701.
- Sudher, K.P., Goasin, A.K., Ramasastri, K.S., 2002. A data-driven algorithm for constructing artificial neural network rainfall-runoff models. *Hydrological Processes* 16, 1325–1330.
- Szidarovszky, F., Coppola, E., Long, J., Hall, A., Poulton, M., 2007. A hybrid artificial neural network-numerical model for groundwater problems. *Ground Water* 45 (5), 590–600.
- Takagi, T., Sugeno, M., 1985. Fuzzy identification of systems and its application to modeling and control. *IEEE Transactions on System, Man and Cybernetics* 15 (1), 116–132.
- Todd, D.K., Mays, L.W., 2005. *Groundwater Hydrology*, Third Revision John Wiley and Sons Inc. 636p.
- Vapnik, V.N., 1995. *The Nature of Statistical Learning Theory*. Springer-Verlag, New York, USA.
- Vapnik, V.N., 1998. *Statistical Learning Theory*. Wiley, New York, USA.
- Vernieuwe, H., Georgieva, O., De Baets, B., Pauwels, V.R.N., Verhoest, N.E.C., De Troch, F.P., 2005. Comparison of data-driven Takagi-Sugeno models of rainfall-discharge dynamics. *Journal of Hydrology* 302 (1–4), 173–186.
- Yoon, H., Hyun, Y., Lee, K.K., 2007. Forecasting solute breakthrough curves through the unsaturated zone using artificial neural networks. *Journal of Hydrology* 335, 68–77.
- Yoon, H., Jun, S.C., Hyun, Y., Bae, G.O., Lee, K.K., 2010. A comparative study of artificial neural networks and support vector machines for predicting groundwater levels in a coastal aquifer. *Journal of Hydrology* doi: 10.1016/j. hydrol. 2010. 11. 002.